Laboratory or sample labeling errors were thought to be responsible for this discrepancy. Of note, in their analysis, Coyne et al. also reported a similar percentage (30%) (13).

Reduced blood processing was due to difficulties with needle placement. Despite adequate staff training and commitment, four (4) cases of needle malposition (reversed needles) were identified. This was observed in three synthetic grafts and an upper arm native fistula. A complete knowledge of the position and direction of flow in an AV access is fundamental for the nursing staff in order to insert the needles in the appropriate place. A simple drawing of an AV access and the direction of its blood flow is highly recommended for every patient's dialysis chart.

In this study, we also investigated higher-than-expected values of Kt/V. These values were always due to false postdialysis sampling as blood was drawn from the venous line of the dialysis circuit leading to low urea concentration and higher Kt/V. This is easy to identify as the postdialysis urea value is extremely low and the calculated Kt/V is unexpectedly high (Table 1, patient 2).

In conclusion, the results of this study demonstrate that lower-than-expected Kt/V values are often due to reduced blood processing (shorter dialysis, lower blood flow, and recirculation) and higher due to inaccurate postdialysis sampling. Although the percentage was rather low, it should not be neglected. Dialysis flow sheets from the testing days should be carefully evaluated in order to identify apparent reasons for abnormal values. The nursing staff should also be trained and familiar with urea kinetic modeling and blood sampling. Abnormal values of Kt/V should always be repeated as soon as possible. Any possible pitfall in Kt/V measurements should be investigated before changing dialysis prescription in a stable HD patient.

Acknowledgment: The authors would like to thank Dr. Arif Asif, Miami, FL, USA, for his careful manuscript review and constructive comments.

REFERENCES

1. Gotch FA, Srgent JA. A mechanistic analysis of the National Cooperative Dialysis Study (NCDS). *Kidney Int* 1985;28:526–34.
2. Gotch FA, Levin NW, Port FK. Clinical outcome relative to the dose of dialysis is not what you think: the fallacy of the mean. *Am J Kidney Dis* 1997;30:1–15.
3. Port FK, Ashby VB, Dhingra RK. Dialysis dose and body mass index are strongly associated with survival in hemodialysis patients. *J Am Soc Nephrol* 2002;13:1061–6.
4. Held PJ, Port FK, Wolfe RA. The dose of hemodialysis and patient mortality. *Kidney Int* 1996;50:550–6.
5. National Kidney Foundation. K/DOQI clinical practice guidelines for hemodialysis adequacy: update 2000. *Am J Kidney Dis* 2001;37:S7–S64.
6. Eknoyan G, Beck GJ, Cheung AK, The Hemodialysis (HEMO) Study Group. Effect of dialysis dose and membrane flux in maintenance hemodialysis. *N Engl J Med* 2002;347: 2010–9.
7. Port FK, Pisoni RL, Bragg-Gresham JL. DOPPS estimates of patient life years attributable to modifiable hemodialysis treatment practices in the United States. *Blood Purif* 2004;22:175–80.
8. Port FK, Wolfe RA, Hulbert-Shearon TE. High dialysis dose is associated with lower mortality among women but not among men. *Am J Kidney Dis* 2004;43:1014–23.
9. Parker TF, Husni L, Huang W. Survival of hemodialysis patients in the United States is improved with a great quantity of dialysis. *Am J Kidney Dis* 1994;23:670–80.
10. Rocco MV, Burkart JM. Prevalence of missed treatments and early sign-offs in hemodialysis patients. *J Am Soc Nephrol* 1993;4:1178–83.
11. Pederson WC, Dunlay R, Llach F. Two-needle calculation of recirculation compared with the standard three-needle method. *Clin Nephrol* 1990;33:203–6.
12. Delmez JA, Weerts CA, Hasamear PD, Windus DW. Severe dialyzer dysfunction undetectable by standard reprocessing validation tests. *Kidney Int* 1989;36:478–84.
13. Coyne DW, Delmez J, Spence G, Windus DW. Impaired delivery of hemodialysis prescriptions: an analysis of causes and an approach to evaluation. *J Am Soc Nephrol* 1997;8:1315–8.
14. Daugirdas JT. Rapid methods of estimating Kt/V: three formulas compared. *ASAIO Trans* 1990;36:362–4.
15. Parker TF. Trends and concepts in the preparation and delivery of dialysis in the United States. *Semin Nephrol* 1992;12:267–75.
16. Sargent JA. Shortfalls in the delivery of dialysis. *Am J Kidney Dis* 1990;15:500–10.
17. Seghal AR, Snow RJ, Singer ME, et al. Barriers to adequate delivery of hemodialysis. *Am J Kidney Dis* 1998;31:593–601.
18. Palevsky PM, Washington MS, Stevenson JA, et al. Barriers to the delivery of adequate hemodialysis in ESRD Network 4. *Adv Ren Replace Ther* 2000;7(Suppl. 1):S11–20.

Hemodynamic Support With the Pulsatile Catheter Pump in a Sheep Model of Acute Heart Failure

**Zhicheng Li, ‡Y. John Gu, *Qing Ye, * Shaofei Cheng, *Weijun Wang, *Min Tang, *Xiaogang Zhao, ‡Gerhard Rakhorst, and *Changzhi Chen*
**Department of Cardiothoracic Surgery, Ren Ji Hospital affiliated with the Shanghai Jiaotong University School of Medicine, Shanghai, China; and ‡Department of Biomedical Engineering, Groningen University Medical Center, the Netherlands*

Abstract: This study was aimed to mimic clinical heart failure (HF) conditions and to assess the effect of pulsatile

Received September 2005; revised April 2006.

Address correspondence and reprint requests to Dr. Changzhi Chen, Department of Cardiothoracic Surgery, Ren Ji Hospital, Shanghai Jiaotong University School of Medicine, 1630, Dongfang Road, Pudong District, Shanghai 200127, China. E-mail: changzhi6@hotmail.com

catheter (PUCA) pump support on hemodynamics and tissue perfusion in a sheep model of acute HF. In 14 sheep, HF was induced by partial occluding the middle left circumflex coronary artery combined with pacemaker-induced tachycardia. PUCA pump was then activated to support the HF for 3 h. Hemodynamic parameters were recorded at baseline, HF, and then every 30 min during experiments. Blood samples were taken in carotid artery (CA), pulmonary artery (PA), and coronary sinus (CS) for the determination of oxygen saturation (SO_2) and lactate concentration as markers of tissue perfusion. Results showed that HF model was induced successfully in 10 sheep and failed in four sheep due to refractory ventricular fibrillation. PUCA pump support was successful in seven out of 10 sheep for 3 h. Three cases failed due to technical problems. After HF ($n = 10$), cardiac output (CO) was decreased from 3.7 ± 0.5 to 2.0 ± 0.5 L/min ($P < 0.001$). Mean arterial pressure (MAP) was lowered from 116.1 ± 14.2 to 68.1 ± 14.7 mm Hg ($P < 0.001$). In seven sheep supported with PUCA pump, MAP rose from 68.9 ± 15.2 to 94.7 ± 14.7 mm Hg ($P = 0.005$), systolic blood pressure increased from 86.6 ± 17.0 to 112.6 ± 17.1 mm Hg ($P = 0.009$), and diastolic blood pressure increased from 57.7 ± 12.6 to 79.9 ± 13.9 mm Hg ($P = 0.011$). CO remained at about 2.0 L/min. SO_2 in CA, PA, and CS decreased significantly after HF ($P < 0.001$), with an increase after support (compared with HF, $P < 0.001$, 0.066 and 0.114, respectively). Lactate concentrations increased gradually in CA, PA, and CS toward the end of experiments without difference among different sampling sites. This HF model in sheep is simple, easy to manipulate, reproducible and reflecting clinical HF conditions. PUCA pump can maintain the hemodynamic status for 3 h in this acute HF model. **Key Words:** Left ventricular assist device—Catheter pump—Heart failure—Sheep.

Intra-aortic balloon pump (IABP) has been widely used during the perioperative period to support patients with low cardiac output (CO). The use of the IABP has continued to increase, particularly over the past decade with the expansion of interventional cardiology, and the increasing age and acuity of cardiac surgical patients (1,2). However, IABP can improve CO by only 10–20%, and thus is inadequate in cases requiring large doses of inotropic agents (3,4). Patients with profound hemodynamic compromise persisting after IABP insertion will likely survive only with a ventricular assist device (VAD) (2,5). Large-scale blood pumps can generate higher pump flow but they are usually expensive and require thoracotomy and sophisticated cannulation. Thus, their clinical application is limited. Pulsatile catheter (PUCA) pump is a new device between IABP and VAD, which is capable of generating higher pump flow than IABP does (6). It not only provides direct left ventricle (LV) unloading effect, but also augments the aortic pressure which in turn increases the coronary flow. This study was aimed (i) to develop a sheep model of acute heart failure (HF) to mimic the clinical conditions and (ii) to assess the effect of PUCA pump support on hemodynamics and tissue perfusion in this sheep model of acute HF.

MATERIALS AND METHODS

The PUCA pump system consists of a 40-cm-long, large bore (21 Fr.) thin-walled nickel-titanium reinforced indwelling catheter and an external transparent membrane pump, which can be activated from any commercially available IABP driver. In the distal end of the catheter, a combined inflow and outflow valve is integrated in the catheter wall. The tip of the catheter similar to a bird cage is integrated into the catheter wall, which aspirates blood from the LV through it when the membrane pump is driven pneumatically by the IABP driver. When the tip of the catheter is positioned in the LV, the pump valve should be located a few centimeters proximally from the native aortic valve. During aspiration, the valve guides the blood from the LV to the membrane pump, and the blood is then ejected through the same catheter into the aorta when it meets the pump valve (Fig. 1). In this study, the pump was driven by an Arrow ACAT1 IABP driver (Arrow International, Reading, PA, USA).

The experiments were conducted in 14 sheep with a mean body weight of 36.8 ± 2.9 kg (range 32~42 kg).

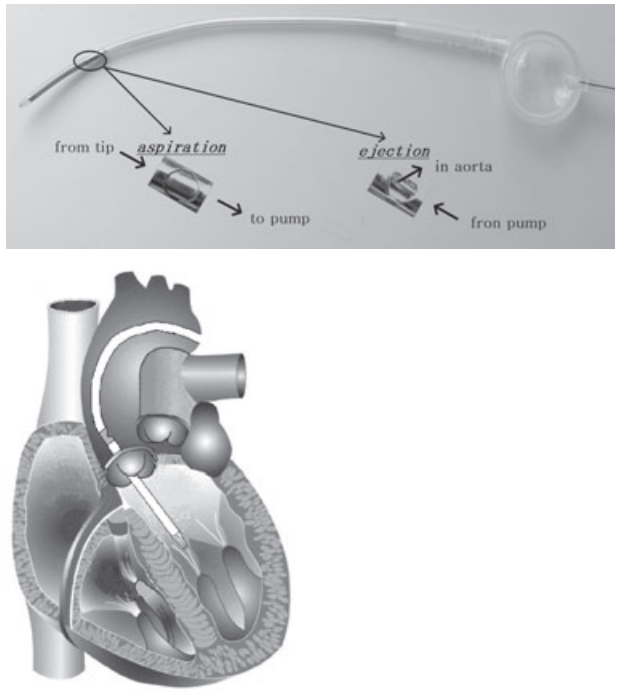

FIG. 1. Picture of the 21 Fr. open-chest version of the pulsatile catheter and 40-mL membrane pump (PUCA pump) with a detailed drawing of the tilting valve, and the schematic drawing of the PUCA positioned in the LV.

All animal experiments were performed according to the rules of the Ethical Committee on Animal Research at the Shanghai Jiaotong University, School of Medicine and conducted in compliance with the Declaration of Helsinki guidelines for the care and use of animals in research. Anesthesia was induced with 10~20 mg/kg of ketamine given intramuscularly. The sheep were ventilated with a Dräger breathing machine (Model 10348, Dräger, Lubeck, Germany). Anesthesia was maintained with a continuous infusion of ketamine and midazolam. Continuous electrocardiograms were recorded from standard limb leads on a Hewlett Packard monitor 54S (Hewlett-Packard, Palo Alto, CA, USA). The sheep were put at right recumbent position on the table. A pressure line was introduced into the left carotid artery (CA) for monitoring systemic arterial blood pressure including systolic blood pressure (SBP), diastolic blood pressure (DBP), and mean arterial pressure (MAP) and obtaining arterial blood gas samples. The blood gas was analyzed by ABL 5050 (Radiometer, Copenhagen, Denmark). A catheter was inserted into the right ventricle through the left external jugular vein for right ventricular end-diastolic pressure (RVEDP) recording. A Swan-Ganz catheter was positioned into the pulmonary artery (PA) via the left femoral vein for CO measurements by a CCO-Baxter Vigilance computer (Vigilance system SvO2/CCO, Baxter Edwards Laboratories, Irvine, CA, USA) and for measuring the central venous pressure (CVP) as well as for blood sampling. A left thoracotomy was performed through the fourth intercostal space. The lung was gently retracted, and the left azygos vein was ligated. To facilitate the collection of blood samples from the coronary sinus (CS) for measurements of oxygen saturation (SO_2) and lactate concentration, cannulation of the left azygos vein was performed (Fig. 2A). The pericardium was thus opened and sewn to the wound edge. Left atrial pressure (LAP) and left ventricular end-diastolic pressure (LVEDP) lines were inserted, respectively, through the left atrial appendage. All pressure lines and cannulae were filled with heparin solution (5000 IU/100 mL 0.9% saline solution).

Before the insertion of the PUCA pump catheter, heparin was given systemically at a dosage of 1.5 mg/kg of body weight. The activated clotting time was then kept around 300 s. A purse string suture was made on the descending thoracic aorta just beyond the subclavian artery. The PUCA pump catheter was inserted into the aorta through a stab wound in the center of the purse string. Its tip was then guided into the LV through the aortic valve using a guide wire and a cardiac catheter. The catheter was used for monitoring the pressure and positioning as described

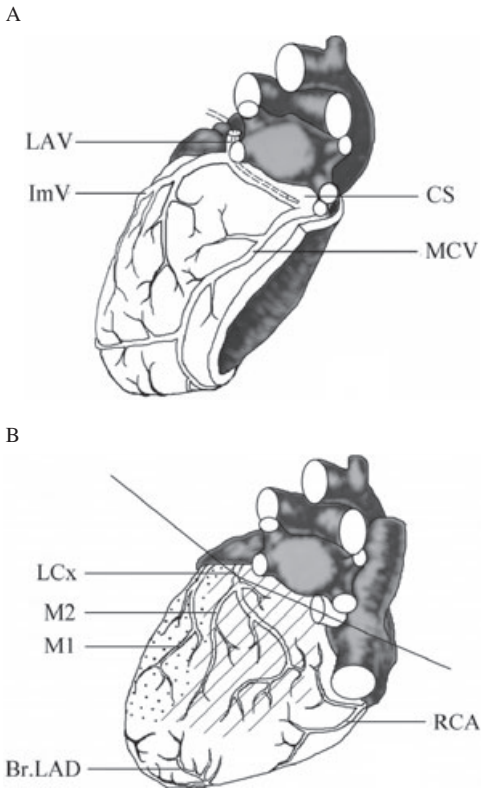

FIG. 2. (A) The venous drainage of LV in sheep and cannulation of the left azygos vein. (B) Posterior view of an arterial diagram of ovine heart and site of partial occlusion of LCx. Crosshatched area represents the flow distribution of the middle LCx. The stippled area depicts the distribution of M1. The stippled and crosshatched areas depict the distribution of LCx. LAV, left azygos vein; ImV, intermediate branch of the great cardiac vein; CS, coronary sinus; MCV, middle cardiac vein; LCx, circumflex branch of left coronary artery with marginal branches labeled M1 and M2; RCA, right coronary artery; Br.LAD, apical branches of LAD.

previously (6). Tourniquets were tightened to control bleeding. The catheter was de-aired and connected to a 40-mL single-pore primed membrane pump (heparin 5000 IU/200 mL 0.9% saline solution). A pair of pacing leads was attached to the myocardium and connected to an external pacemaker (Medtronic 5330, Minneapolis, MN, USA) to control the heart rate. To prevent ventricular arrhythmias, 50-mg Lidocaine was given as a slow intravenous bolus before the left circumflex coronary artery (LCx) was partially occluded.

Baseline hemodynamic parameters and blood samples were taken after 10 min of stabilization in hemodynamics with the said operative procedure finished. HF model was induced by partially occluding the middle LCx combined with pacemaker-induced tachycardia (Fig. 2B). After a period of 15 min for stability, further cardiac dysfunction was

induced by intermittent stepwise pacemaker-induced tachycardia, which was achieved by triggering the heart rate from 120 to 180 beats/min with an increment of 10 beats/min for every 5 min until the establishment of HF. Myocardial ischemia was evidenced by electrocardiographic changes, including ST-segment elevation and T wave inversion. The following criteria were set to define HF: a decrease of ≥25% in MAP, combined with a decrease of ≥25% in CO from the baseline. About 10 min after successful induction of ischemic HF, hemodynamic parameters were recorded and blood samples were taken as scheduled. The PUCA pump was then activated to support the hemodynamics for 3 h. Pump frequency was set at a fixed rate of 80 beats/min. Further recording on hemodynamic parameters was taken every 30 min. Blood samples were also taken every 15 min, then every 30 and 180 min. SO_2 and lactate concentration was measured in CA, PA, and CS, which were used as tissue perfusion markers.

Mean and SD were derived for each parameter analyzed. Analysis of variance (ANOVA) was applied for the evaluation of the effect of time on a parameter's profile and comparisons were done by least significant difference. Statistical significance was reached at $P < 0.05$.

RESULTS

HF model was induced successfully in 10 sheep and failed in four sheep due to refractory ventricular fibrillation resulting from occluding the middle LCx combined with pacemaker-induced tachycardia. In 10 HF sheep, the measured hemodynamic results are listed in Table 1. CO decreased from 3.7 ± 0.5 to 2.0 ± 0.5 L/min ($P < 0.001$). MAP lowed from 116.1 ± 14.2 to 68.1 ± 14.7 mm Hg ($P < 0.001$). CVP rose from 7.1 ± 2.2 to 10.7 ± 3.5 mm Hg ($P < 0.05$), and LAP increased from 8.1 ± 2.1 to 12.0 ± 4.6 mm Hg ($P < 0.01$).

PUCA pump support was succeeded in seven of 10 sheep for 3 h. For the three failed sheep, one had a sudden cardiac arrest and refractory ventricular fibrillation which could not be resuscitated following 1-h PUCA pump support. The other two cases had technical problems in cannulation. Hemodynamic parameters are depicted in Table 2 (ANOVA, $P < 0.001$, <0.001, <0.001, <0.001, 0.886, 0.969, 0.806, and 0.533, respectively). During the 3-h support, MAP rose from 68.9 ± 15.2 to 94.7 ± 14.7 mm Hg ($P = 0.005$), SBP increased from 86.6 ± 17.0 to 112.6 ± 17.1 mm Hg ($P = 0.009$), and DBP increased from 57.7 ± 12.6 to 79.9 ± 13.9 mm Hg ($P = 0.011$). No significant change was found in CO, CVP, RVEDP, LAP, and LVEDP. However, in one sheep that successfully developed HF but did not receive effective support due to technical problems in cannulation, MAP and CO dropped, respectively, to <20 mm Hg and <1.0 L/min after 3 h, which was much worse than the supported animals.

TABLE 1. *Hemodynamic parameters at baseline and after HF induction (n = 10)*

	Baseline	HF	P
CO (L/min)	3.7 ± 0.5	2.0 ± 0.5	<0.001
SBP (mm Hg)	133.6 ± 10.2	86.0 ± 15.8	<0.001
DBP (mm Hg)	106.5 ± 15.8	58.1 ± 13.4	<0.001
MAP (mm Hg)	116.1 ± 14.2	68.1 ± 14.7	<0.001
CVP (mm Hg)	7.1 ± 2.2	10.7 ± 3.5	0.022
RVEDP (mm Hg)	6.1 ± 3.6	9.9 ± 4.4	0.050
LAP (mm Hg)	8.1 ± 2.1	12.0 ± 4.6	0.008
LVEDP (mm Hg)	8.5 ± 4.2	13.1 ± 10.6	0.190

Mean values with SD.

The values of SO_2 in CA, PA, and CS decreased significantly after HF. They were 99.8 ± 0.3, 82.2 ± 1.4, and 80.9 ± 2.1% for baseline, while 95.0 ± 0.6, 70.5 ± 2.6, and 66.5 ± 2.4% for HF ($P < 0.001$, <0.001, and <0.001, respectively). By supporting with PUCA pump, they rose to 99.5 ± 0.4, 74.4 ± 3.2, and 71.1 ± 6.7% at 180-min time point (compared with HF, $P < 0.001$, 0.066, and 0.114, respectively) (ANOVA, $P < 0.001$, <0.001, and <0.001, respectively) (Table 3). Lactate concentrations in CA, PA, and CS varied significantly. They were 3.3 ± 0.6, 3.1 ± 0.5, and 3.1 ± 0.5 mM for baseline, and 3.4 ± 0.5, 3.3 ± 0.5, and 3.2 ± 0.5 mM for HF (compared with baseline, $P = 0.826$, 0.579, and 0.617, respectively). However, when at 180 min, they increased to 4.1 ± 0.8, 4.2 ± 0.9, and 4.1 ± 0.9 mM (compared with baseline, $P = 0.004$, <0.001, and 0.001, respectively; compared with HF, $P = 0.007$, 0.001, and 0.003, respectively) (ANOVA, $P = 0.025$, 0.001, and 0.002, respectively). Looking at lactate values in CA, PA, and CS at the same time points, they were very close (ANOVA, $P = 0.632$, 0.787, 0.987, 0.647, 0.507, 0.662, 0.906, 0.986, and 0.981, respectively) (Table 4).

DISCUSSION

HF may be induced experimentally by overloading pressure or volume, myocardial infarction, or pacemaker-induced tachycardia. Among these methods, myocardial infarction is considered the most suitable method for assessing new circulatory assist devices (7,8). The easiest way to induce myocardial infarction and the subsequent HF seems to be a coronary occlusion by ligature or injection of

TABLE 2. *Hemodynamic parameters before and during PUCA pump support (n = 7)*

			Support time (min)					
	B	HF	30	60	90	120	150	180
CO (L/min)	3.7 ± 0.5	2.2 ± 0.4*	2.0 ± 0.4*	2.2 ± 0.7*	1.8 ± 0.4*	2.4 ± 0.7*	2.1 ± 0.7*	2.3 ± 0.7*
SBP (mm Hg)	133.9 ± 11.6	86.6 ± 17.0*	93.6 ± 20.1*	95.6 ± 21.2*	107.4 ± 27.2*,**	108.0 ± 10.6*,**	110.7 ± 11.0*,**	112.6 ± 17.1*,**
DBP (mm Hg)	106.6 ± 19.0	57.7 ± 12.6*	63.0 ± 14.7*	64.9 ± 21.1*	78.7 ± 18.0*,**	79.1 ± 8.8*,**	80.0 ± 13.8*,**	79.9 ± 13.9*,**
MAP (mm Hg)	115.9 ± 17.0	68.9 ± 15.2*	73.3 ± 16.2*	77.7 ± 22.5*	90.3 ± 21.3*,**	92.1 ± 7.6*,**	92.9 ± 10.8*,**	94.7 ± 14.7*,**
CVP (mm Hg)	7.4 ± 2.2	9.7 ± 3.2	11.3 ± 4.0	10.4 ± 3.5	10.6 ± 5.9	9.7 ± 5.6	9.1 ± 6.7	8.6 ± 6.7
RVEDP (mm Hg)	6.0 ± 4.3	8.9 ± 3.3	7.6 ± 3.8	7.4 ± 3.4	8.1 ± 4.9	7.6 ± 5.1	9.9 ± 9.7	8.9 ± 10.2
LAP (mm Hg)	8.0 ± 2.2	10.6 ± 4.2	15.6 ± 14.6	12.4 ± 6.2	13.9 ± 8.2	11.9 ± 6.4	13.4 ± 10.9	14.4 ± 10.3
LVEDP (mm Hg)	8.0 ± 3.4	12.4 ± 12.2	8.6 ± 7.0	8.0 ± 7.0	11.9 ± 7.2	13.4 ± 4.9	14.6 ± 6.8	14.4 ± 11.3

Mean values with SD. Compared with baseline (B): *$P < 0.05$; compared with HF: **$P < 0.05$.

TABLE 3. *Oxygen saturation before and during PUCA pump support (n = 7)*

			Support time (min)						
	B	HF	15	45	75	105	135	165	180
CA (%)	99.8 ± 0.3	95.0 ± 0.6*	96.0 ± 1.2*,**	96.8 ± 1.7*,**	97.6 ± 1.6*,**	98.0 ± 1.6*,**	98.4 ± 1.4*,**	98.9 ± 1.1**	99.5 ± 0.4**
PA (%)	82.2 ± 1.4	70.5 ± 2.6*	71.5 ± 2.0*	68.7 ± 3.6*	68.6 ± 4.3*	73.8 ± 4.8*	74.5 ± 6.7*	73.5 ± 4.4*	74.4 ± 3.2*
CS (%)	80.9 ± 2.1	66.5 ± 2.4*	70.2 ± 4.1*	67.3 ± 2.7*	66.7 ± 3.6*	72.5 ± 8.1*,**	71.1 ± 6.7*	71.0 ± 7.3*	71.1 ± 6.7*

Mean values with SD. Compared with baseline (B): *$P < 0.05$; compared with HF: **$P < 0.05$.

TABLE 4. *Blood lactate concentration before and during PUCA pump support (n = 7)*

			Support time (min)							
	B	HF	15	45	75	105	135	165	180
CA (mmol/L)	3.3 ± 0.6	3.4 ± 0.5	3.8 ± 0.3	3.8 ± 0.2	3.8 ± 0.3	4.0 ± 0.3***	4.0 ± 0.5***	4.1 ± 0.6***	4.1 ± 0.8***
PA (mmol/L)	3.1 ± 0.5	3.3 ± 0.5	3.8 ± 0.3***	3.8 ± 0.2***	3.9 ± 0.2***	3.9 ± 0.3***	4.0 ± 0.5***	4.1 ± 0.6***	4.2 ± 0.9***
CS (mmol/L)	3.1 ± 0.5	3.2 ± 0.5	3.8 ± 0.4***	3.8 ± 0.1*	3.7 ± 0.3*	4.1 ± 0.5***	3.9 ± 0.5***	4.1 ± 0.7***	4.1 ± 0.9***

Mean values with SD. Compared with baseline (B): $^{*}P < 0.05$; compared with HF: $^{**}P < 0.05$.

microspheres. However, because of the background of normal coronary arteries, it is extremely difficult to obtain stable HF after acute coronary occlusion in animals, particularly in larger species. Either cardiogenic shock or compensatory changes may immediately happen after coronary occlusion. Therefore HF, an intermediate situation, is difficult to establish (7,9). However, the major problem with the rapid pacing-induced HF model is that biochemical and hemodynamic alterations revert nearly to normal values soon after pacing is ceased (9–11). Because of these, we tried to develop HF with a coronary stenosis, that is, partial instead of total occlusion of the artery. The advantage of this method is that hearts with normal coronary arteries have the ability to adapt ischemic process. In this study, we used sheep as experimental animals because sheep are a widely available large animal and can withstand operation well. In addition, in sheep, LV myocardium, including the septum, is almost exclusively perfused by the left coronary artery, whereas the venous drainage of the LV can be totally confined to the CS after experimental ligation of the left azygos vein (Fig. 2A). This characteristic allows cannulation of the left azygos vein to facilitate the collection of blood samples from the CS for the study of LV myocardial metabolism and oxygen consumption (12,13).

The ideal model should be safe, easy to manipulate, and reproducible as well as reflecting clinical HF conditions. As reported by Mihaylov and associates (14), it is hard to control the degree of the coronary stenosis when a tourniquet is placed around the coronary artery. Therefore, they developed a Delrin screw-type constrictor to solve this problem. Compared with their relatively complicated method, in our experiment, the degree of the coronary stenosis was shown by the degree of myocardial ischemia which was evidenced by electrocardiographic changes. Therefore, it is easier to manipulate. From previous reports (9,14,15), HF was usually caused by stenosis or occlusion of the proximal LCx. However, as we found earlier (16), ventricular arrhythmias and ventricular fibrillation happened early and often led to death. Too large an area of myocardial infarction involving the posterior septum, the inferior and lateral walls, the junction of the right ventricle with the posterior and right walls of LV (12), and the lack of collateral vessels in sheep may be responsible for the early deaths. In this study, partial occlusion of the middle LCx was applied to avoid this problem (Fig. 2B).

As known in literature, the Hemopump can directly unload LV through aspirating the blood from the left ventricular cavity and expelling it in the ascending aorta (17). In contrast to Hemopump, IABP exerts its

effect by volume displacement. It has two principle effects; the first is to augment coronary blood flow, and thus myocardial oxygen supply, by increasing diastolic perfusion pressure. The blood displaced during balloon inflation reduces ventricular work by reducing afterload with rapid balloon deflation in systole, thus decreasing myocardial oxygen consumption (18). The PUCA pump in fact combines the direct LV-unloading effect of the Hemopump with the counterpulsation effect of IABP (17,19). In this study, a significant increase in MAP, SBP, and DBP was found during PUCA pump support, which indicated the improvement in hemodynamics and elevation in perfusion pressure for the failing heart. However, there was no significant improvement in CO and the filling pressures such as LAP and LVEDP, which was likely due to the severity of this HF model so that the natural heart had contributed little during this initial 3 h of support. Moreover, under such an HF condition that the retained LV volume of the failing heart was mechanically suctioned by the catheter pump, the Frank-Starling mechanism might not be function well to increase CO. Furthermore, it was not certain whether the asynchronous ejection mode between the fixed pumping rate (80 beats/min) and the varying heart rate would have a negative effect on the overall cardiac performance (20).

The blood lactate level following surgery was usually elevated to 40~60 mg/dL (4.4~6.7 mM) and took about 6~8 h to return to normal (21). In our study, the lactate level increased gradually toward the end of experiment, indicating that the high level of blood lactate was fundamentally ascribed to surgical operation. In contrast, we found an almost similar level of lactate concentrations in the CA, PA, and CS. Actually, a higher concentration of lactate would be expected in CS than in CA and PA should any anaerobic metabolism occur in the ischemic myocardium as a result of inadequate perfusion (22). In this context, PUCA support may have improved myocardium perfusion. From our results, SO_2 appeared more sensitive than blood lactate to changes in hemodynamics. Robison and associates (23) indicated that anaerobic metabolism was demonstrated by the rise in the arterial lactate concentration greater than 1.0 mM and a reduction of SO_2 to less than 40%. In contrast to this, Takatani (21) suggested that an SO_2 level of 10~15% in PA seemed to be the lower anaerobic threshold. As discussed earlier, and taking our results into consideration, blood gas parameters and blood lactate levels reflected adequate tissue perfusion with the PUCA pump support after HF.

In conclusion, we have developed an ischemic HF model in sheep by partially occluding the middle LCx combined with pacemaker-induced tachycardia. This HF model in sheep is simple, easy to manipulate, reproducible and reflecting clinical HF conditions. PUCA pump can maintain the hemodynamics for 3 h in this acute HF model and provide sufficient blood flow to ensure adequate tissue perfusion.

Acknowledgments: This study was funded by a research grant of the Renji Hospital, Jiaotong University School of Medicine, Shanghai, China. The authors wish to express their gratitude to Dr. JP van Loon from IntraVasc BV, Groningen, for supplying the PUCA pump and to Xuejun Wu, Gulan Zhang, and Xiaomei Wang for their assistance in animal experiments.

REFERENCES

1. Christenson JT, Badel P, Simonet F, Schmuziger M. Preoperative intraaortic balloon pump enhances cardiac performance and improves the outcome of redo CABG. *Ann Thorac Surg* 1997;64:1237–44.
2. Torchiana DF, Hirsch G, Buckley MJ, et al. Intraaortic balloon pumping for cardiac support: trends in practice and outcome, 1968–1995. *J Thorac Cardiovasc Surg* 1997;113:758–64; discussion 764–9.
3. Maccioli G, Lucas W, Norfleet E. The intra-aortic balloon pump: a review. *J Cardiothorac Anesth* 1988;2:365–73.
4. Naunheim KS, Swartz MT, Pennington DG, et al. Intraaortic balloon pumping in patients requiring cardiac operations. Risk analysis and long-term follow-up. *J Thorac Cardiovasc Surg* 1992;104:1654–61;discussion 1660–1.
5. Baldwin RT, Slogoff S, Noon GP, et al. A model to predict survival at time of postcardiotomy intraaortic balloon pump insertion. *Ann Thorac Surg* 1993;55:908–13.
6. Mihaylov D, Kik C, Elstrodt J, Verkerke GJ, Blanksma PK, Rakhorst G. Development of a new introduction technique for the pulsatile catheter pump. *Artif Organs* 1997;21:425–7.
7. Smith HJ, Nuttall A. Experimental models of heart failure. *Cardiovasc Res* 1985;19:181–6.
8. Kuroda H, Suga H. Cardiac function of an acute ischemic heart failure model produced by microsphere injection into the left coronary artery. Pressure–Volume relationship as determined by a conductance catheter. *ASAIO J* 1995;41:855–62.
9. Shen YT, Lynch JJ, Shannon RP, Wiedmann RT. A novel heart failure model induced by sequential coronary artery occlusions and tachycardiac stress in awake pigs. *Am J Physiol* 1999;277:H388–98.
10. Larosa G, Armstrong PW, Seeman P, Forster C. Beta adrenoceptor recovery after heart failure in the dog. *Cardiovasc Res* 1993;27:489–93.
11. Moe GW, Stopps TP, Howard RJ, Armstrong PW. Early recovery from heart failure: insights into the pathogenesis of experimental chronic pacing-induced heart failure. *J Lab Clin Med* 1988;112:426–32.
12. Markovitz LJ, Savage EB, Ratcliffe MB, et al. Large animal model of left ventricular aneurysm. *Ann Thorac Surg* 1989;48:838–45.
13. Huang Y, Kawaguchi O, Zeng B, et al. A stable ovine congestive heart failure model. A suitable substrate for left ventricular assist device assessment. *ASAIO J* 1997;43:M408–13.
14. Mihaylov D, Reintke H, Blanksma P, De Jong ED, Elstrodt J, Rakhorst G. Development of acute ischemic heart failure in sheep. *Int J Artif Organs* 2000;23:325–30.
15. Zhang J, Wilke N, Wang Y, et al. Functional and bioenergetic consequences of postinfarction left ventricular remodeling in a

new porcine model. MRI and ^{31}P-MRS Study. *Circulation* 1996;94:1089–100.
16. Li ZC, Chen CZ, Ye Q, et al. The application for pulsatile catheter pump support on cardiac resuscitation in sheep. *Chin J Emerg Med* 2005;14:181–4.
17. Meyns B, Nishimura Y, Racz R, Jashari R, Flameng W. Organ perfusion with Hemopump device assistance with and without intraaortic balloon pumping. *J Thorac Cardiovasc Surg* 1997;114:243–53.
18. Kusiak VM, Goldberg S. Percutaneous intra-aortic balloon counterpulsation. *Cardiovasc Clin* 1985;15:281–302.
19. Mihaylov D, Verkerke GJ, Rakhorst G. Mechanical circulatory support systems—a review. *Technol Health Care* 2000;8: 251–66.
20. Dalby MCD, Banner NR, Tansley P, Grieve LA, Partridge J, Yacoub MH. Left ventricular function during support with an asynchronous pulsatile left ventricular assist device. *J Heart Lung Transplant* 2003;22:292–300.
21. Takatani S. Open-loop analysis of circulatory system in awake live animals: relations between mixed venous saturation (SvO2) and hemodynamic parameters. *Artif Organs* 1993;17: 79–91.
22. Miyama M, Dihmis WC, Deleuze PH, et al. The gastrointestinal tract: an underestimated organ as demonstrated in an experimental LVAD pig model. *Ann Thorac Surg* 1996;61:817–22.
23. Robison PD, Pantalos GM, Long JW Jr, et al. Measurement of oxygen consumption and arterial-venous oxygen saturation following total artificial heart implantation. *Int J Artif Organs* 1993;16:135–40.

A Flow Sensor Suitable for Use With Split-flow Ventilation—First Preclinical Data

*Martin Wald, *Valerie Jeitler, †Karin Lawrenz, *Manfred Weninger, *Arnold Pollak, and *Lieselotte Kirchner

*Division of Neonatology and Intensive Care, Department of Pediatrics, Medical University of Vienna, Austria; and †Department of Pediatric Surgery, University Hospital of Munster, Germany

Abstract: Volutrauma caused by artificial ventilation represents a major morbidity risk for premature infants. Our working group has recently developed an innovative "split-flow ventilation" system aiming at the reduction of tidal volumes (TVs). The main problem for the practical use of this system is the fact that conventional measurements of commercially available flow sensors are distorted by the split flow. In this study, we present the first preclinical data from testing an adapted flow sensor combination recognizing the split flow. A preterm infant test lung was conventionally ventilated, modified by insertion of a split-flow line. In addition to the customary flow sensor (FS-1), a second flow sensor (FS-2) was integrated into the split-flow line, and a third (FS-3) was placed at the exit of the test lung for reference measurements. The signals of all three flow sensors were read and processed by a computer. The program was set to graphically add up flow curves 1, 2, and 3 during one ventilation loop. After 10 runs, a mean curve of FS-1+2 was calculated and compared to the mean curve of FS-3. Furthermore, the mean TV of 10 runs measured by FS-1+2 was calculated and compared with the mean TV calculated by FS-3. The summation curve FS-1+2 proved identical to the reference curve FS-3. FS-1+2 yielded a TV of 6.6 ± 0.01 mL (inspiratory) and 6.7 ± 0.02 mL (expiratory). The corresponding values of FS-3 were 6.5 ± 0.20 mL and 6.6 ± 0.09 mL, respectively. According to our results, the presented flow sensor constellation allows exact flow measurements in the experimental setting and appears suitable for usage in a split-flow ventilation circuit under clinical conditions. **Key Words:** Mechanical ventilation—Very low birth weight infants—Dead space—Volutrauma.

Artificial ventilation of premature infants entails a number of serious side effects. In particular, overexpansion of alveoli by large tidal volumes (TVs) has been proven to contribute significantly to the development of chronic lung disease (1–3).

Since this causal relation has been recognized, efforts have been made to reduce volutrauma by keeping the TV as low as possible (4). A major factor counteracting these endeavors is the "apparatus dead space" (aDS) in which breathing gas is shifted back and forth without taking part in gas exchange.

"Split-flow ventilation" is a method recently invented by our working group which offers a way of functional aDS diminution (5,6). Part of the flow generated by the ventilator is branched off the afferent limb of the ventilation circuit via an additional tube which bypasses the Y-piece and the flow sensor, and rejoins the patient limb at the level of the connection piece of the endotracheal tube (ETT) (Fig. 1). It is mainly during the pause between expiration and inhalation that the bypass or "split" flow fills the flow sensor with fresh breathing gas in retrograde fashion thus washing out its aDS. A major disadvantage of the prototype of this system is the fact that conventional expiratory flow measurement with a flow sensor in the patient limb of the Y-piece yields wrong (too high) values due to the addition of this split flow. In order to overcome this problem, we have inserted an adapted flow sensor combination into the ventilation circuit. This arrangement was tested in an experimental setting. The aim of the study was to demonstrate that with this flow sensor combination, clinical implementation of split-flow ventilation is possible with limited technical support.

Received January 2006; revised March 2006.

Address correspondence and reprint requests to Dr. Lieselotte Kirchner, Division of Neonatology and Intensive Care, Department of Pediatrics, University of Vienna, Währinger Gürtel 18-20, A-1090 Vienna, Austria. E-mail: lieselotte.kirchner@meduniwien.ac.at